

# Particle Clogging in Radial Flow: Microscale Mechanisms

Julio R. Valdes, SPE, San Diego State U., and J. Carlos Santamarina, Georgia Inst. of Technology

## Summary

Fluid-flow-driven particle migration through porous networks reflects the interplay between various particle-level forces, the relative size between migrating particles and pore constrictions, and the spatial variability of the velocity field. Experimental evidence shows that particle migration in radial fluid flow results in self-stabilizing annular clogging patterns when the particle size approaches the constriction size. Conversely, flow localization and flushing instability are observed when the particle size is significantly smaller than the pore-throat size.

## Introduction

Fluid flow through a porous network is often accompanied by the migration of fine particles. This is a common phenomenon in geomaterials (Gruesbeck and Collins, 1982; Ryan and Elimelech 1996), filters (Kenney et al. 1985; Bigno et al. 1994; Bhatia et al. 1998; Reddi et al. 2000), and biological systems (Bonala and Reddi 1998). In certain conditions, massive particle clogging develops, reducing the medium's fluid-transport capacity and thus decreasing productivity (Muecke 1979; Priisholm et al. 1987; Khilar and Fogler 1998). In other cases, particles are flushed out of the medium, yielding an increased fluid conductivity (Kenney and Lau 1985; Skempton and Brogan 1994).

In this study, particle migration and retention are analyzed at the microscale to identify governing particle-level phenomena, with emphasis on mechanical processes rather than electrical interactions, which have been analyzed by previous researchers (e.g., Jones 1964; Cerda 1987; Kia et al. 1987; Sharma and Yortsos 1987; Vaidya and Fogler 1990; Raveendran and Amirtharajah 1995). At the macroscale, clogging and flushing patterns are investigated in radial flow, where the fluid velocity and the forces experienced by migratory particles vary in space.

## Particle-Level Forces

A solid particle within a moving fluid experiences drag, buoyant weight, inertia to motion changes, and electrical interaction forces with nearby pore walls (McDowell-Boyer et al. 1986; Sharma et al. 1992; Herzog et al. 1970). These forces scale with the size of migratory particles  $d_p$  according to power-law equations of the form  $F = \alpha d_p^\beta$  where the exponent is  $\beta=1$  for van der Waals attraction and drag forces,  $\beta=2$  for the inertial force, and  $\beta=3$  for buoyant weight (Note: the inertia to motion changes is estimated for a deceleration from velocity  $v$  to zero within a distance equal to the migratory-particle diameter  $d_p$ ). Therefore, the log-log plot of participating forces vs. particle size,  $\log(F) = \log(\alpha) + \beta \log(d_p)$ , consists of straight lines with different slopes  $\beta$  (Fig. 1). These lines intersect at characteristic particle sizes that define boundaries for different force-control regimes (Santamarina 2002). It can be seen that a certain fluid velocity is required to detach any particle smaller than  $d_p \approx 30 \mu\text{m}$ , because the van der Waals attraction force (which prevails over buoyant weight) scales with particle diameter with the same exponent as the drag force. However, the velocity required to mobilize larger particles is proportional to their buoyant weight ( $\beta=3$ ). In general, the inertial force ( $\beta=2$ ) gains relevance in high-velocity fluid flow and in nonuniform flow regimes near pore constrictions or orifices.

The relative balance among drag force, buoyant weight, and the inertial force is captured in three dimensionless ratios:

$$\text{Ar} = \frac{v\mu}{d_p^2 g \Delta\rho} \text{ (Archimedes) } \dots\dots\dots (1)$$

$$\text{Fr} = \frac{v^2}{d_p g} \text{ (Froude) } \dots\dots\dots (2)$$

$$\text{Re} = \frac{v d_p \rho_f}{\mu} \text{ (Reynolds) } \dots\dots\dots (3)$$

which involve particle size  $d_p$ , fluid velocity  $v$ , dynamic viscosity  $\mu$ , gravity  $g$ , and both particle and fluid mass densities  $\rho_p$  and  $\rho_f$ . The sample calculations displayed in Fig. 1 include the values of these dimensionless ratios at intersection points.

## The Effects of Particle Size, Shape, and Concentration

Particles can be retained at pore constrictions within the pore network. This is clearly the case when particles are larger than pore throats. However, clogging is often observed when the size of migrating particles is smaller than pore throats (Muecke 1979; Sakthivadivel and Einstein 1970; Oyeneyin et al. 1995). This suggests that particles are retained by forming bridges at pore constrictions. Particle-size and -shape effects on bridging were studied using a vertical tube that rests on a bottom plate with a central orifice of diameter  $d_{or}$ . The tube was filled with dry particles (known diameter  $d_p$  and shape), and the plug closing the orifice was removed to allow particle flow. The test was repeated with orifices of different diameter to explore a wide range of  $d_{or}/d_p$  ratios. Three bridging regimes are identified (Fig. 2): no bridging when  $d_{or}/d_p > \delta_{max}$ , intermittent bridge formation when  $\delta_{min} < d_{or}/d_p < \delta_{max}$ , and stable bridge formation when  $d_{or}/d_p < \delta_{min}$ . Clearly, the probability of stable bridge formation decreases as the size of migrating particles  $d_p$  becomes much smaller than the size of the pore throat  $d_{or}$  (Valdes 2002). Furthermore, results show that the characteristic values  $\delta_{min}$  and  $\delta_{max}$  that separate these regimes depend on particle shape, as shown in Fig. 2: Sphericity (vs. ellipticity or flatness), roundness (vs. angularity), and smoothness (vs. roughness). The intermediate regime ( $\delta_{min} < d_{or}/d_p < \delta_{max}$ ) is characterized by intermittent bridge formation and destabilization events. This regime is sensitive to externally imposed vibrations and can benefit from vibration-based unclogging techniques (Beresnev and Johnson 1994).

Bridge formation by dispersed particles within a flowing fluid requires that the N-particles that will form the bridge reach the pore throat almost simultaneously (where N is a function of  $d_o/d_p$ ). It is anticipated that the chances of bridge formation increase as the volume fraction of particles in the pore fluid increases. The effect of volume fraction on bridging was studied with a tube-orifice system similar to the device described previously. Nylon particles were evenly mixed with de-aired saltwater of equal mass density,  $\rho_f = \rho_p$ , to create a stable suspension. The same initial mixture volume was used in all tests. Flow was initiated by unplugging the central orifice. The bridge/pass response was established for various  $d_{or}/d_p$  ratios and volume fractions  $C$ . Fig. 3 shows that the probability of bridging by migrating particles in fluid flow decreases with increasing  $d_{or}/d_p$  and with decreasing volume fraction  $C$ . Furthermore, bridging will eventually take place given enough fluid flow as long as the bridging limiting condition  $d_{or}/d_p < \delta_{min}$  is satisfied.

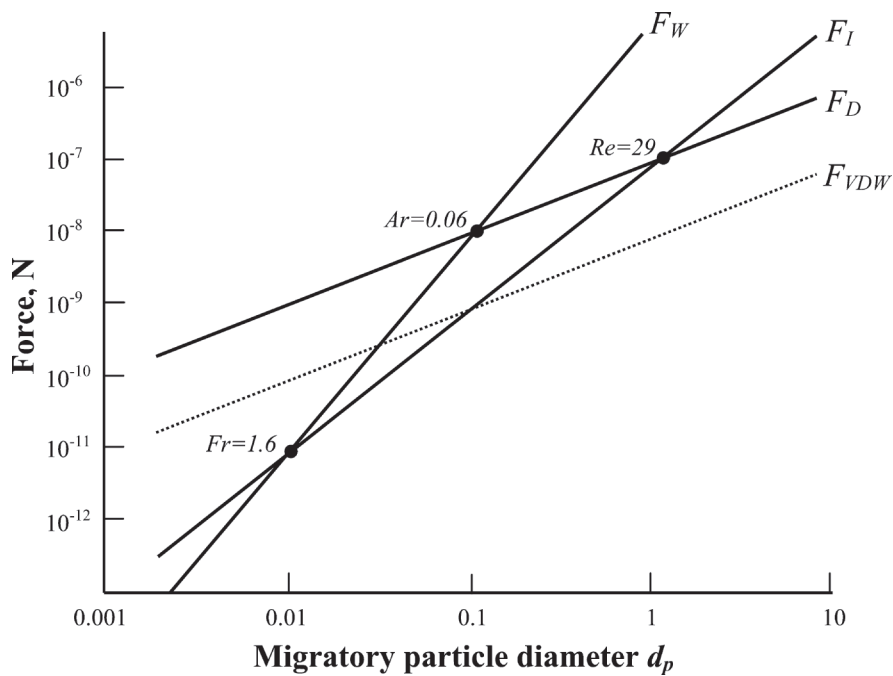


Fig. 1—Forces on a particle within moving fluid: Viscous drag  $F_D$ , van der Waals  $F_{VDW}$ , buoyant weight  $F_W$ , and inertial force  $F_I$ . The following parameters are assumed: Separation from a substrate =  $30 \text{ \AA}$ , Hamaker constant =  $0.09 \times 10^{-20} \text{ J}$ , fluid velocity  $v = 1 \text{ cm/s}$ , dynamic fluid viscosity  $\mu = 1 \text{ cp}$ , particle mass density  $\rho_p = 2.65 \text{ g/cm}^3$ , and fluid mass density  $\rho_f = 1 \text{ gm/cm}^3$ . The dimensionless numbers shown at corresponding intersections are: Archimedes  $Ar$ , Froude  $Fr$ , and Reynolds  $Re$ .

### Retardation and Inertial Effects

The rate of particle transport is inherently lower than the rate of fluid transport (horizontal flow): The difference between fluid and particle velocities gives rise to the drag forces that transport the particles. However, there are additional delays. Previous researchers explored particle-delay mechanisms related to electrical and hydrodynamic interactions among particles and pore walls, and flow-field disruptions near the orifice when the size of the migrating particle  $d_p$  is comparable to the size of the orifice  $d_o$  (Goren and O'Neill 1971; Ramachandran et al. 2000). In this study, we analyze inertial effects, which appear particularly important in a spatially varying velocity field such as radial flow.

Consider a spherical particle with diameter  $d_p$  and mass density  $\rho_p$  entrained in a moving fluid with mass density  $\rho_f \neq \rho_p$ . The particle trajectory is affected by drag, buoyant weight, and the emergent inertial forces in the nonhomogeneous velocity field, as captured in dimensionless ratios  $Ar$ ,  $Fr$ , and  $Re$  (Eqs. 1 through 3; Fig. 1). When  $Fr$  and  $Re$  are high, the entrained particle tends to maintain its trajectory; the particle deviation from fluid-flow lines is aggravated where streamlines curve near the constriction, and the migrating particle often impacts the pore walls. This mechanism is termed "inertial retardation" (Wennberg 1998). On the other hand, when  $Fr$  and  $Ar$  are low, the particle trajectory deviates from the fluid trajectory in the direction of gravity, resulting in "gravity offset"; in this case, the particle may precede the flowing fluid.

These retardation mechanisms were experimentally and numerically studied with single particles to avoid interparticle interactions. The experimental study was conducted using a cylindrical container filled with de-aired oil. First, the particle was released within the fluid and allowed to reach terminal velocity. Then, fluid flow was initiated through a central bottom orifice. The single-particle trajectory was video-recorded and digitized. The trajectory was also predicted with a finite-difference formulation of Newtonian equations, taking drag forces into consideration. Predicted trajectories closely matched the measured trajectories for all tested conditions, which included various initial positions and different relative densities  $\rho_p/\rho_f$ . Selected examples are shown in Fig. 4 [further details can be found in Valdes (2002)]. These results highlight the pronounced effect of the relative mass density  $\rho_p/\rho_f$  on particle trajectories and show that inertial retardation is velocity-field-dependent.

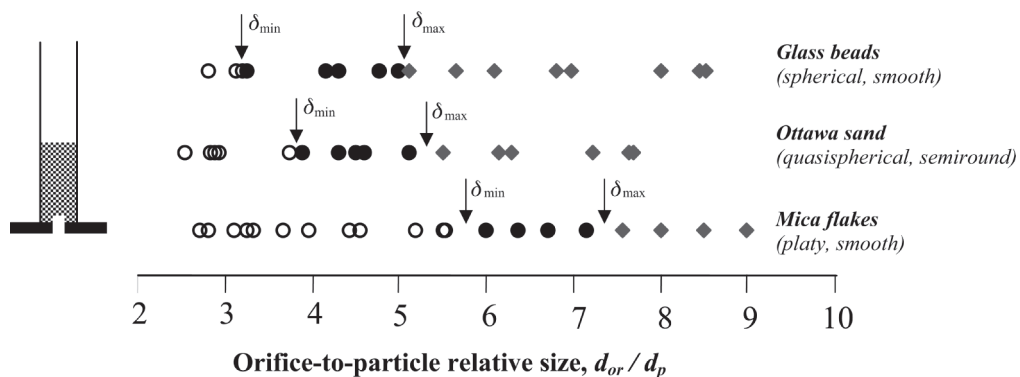


Fig. 2—Particulate bridge formation: Particle shape effect on bridging without fluid flow. Open circles, closed circles, and diamonds represent stable bridges, vibration-sensitive bridges, and no bridges, respectively. The experiment consists of a tube filled with the selected grains placed on top a plate with an orifice of known diameter (see schematic on the left).

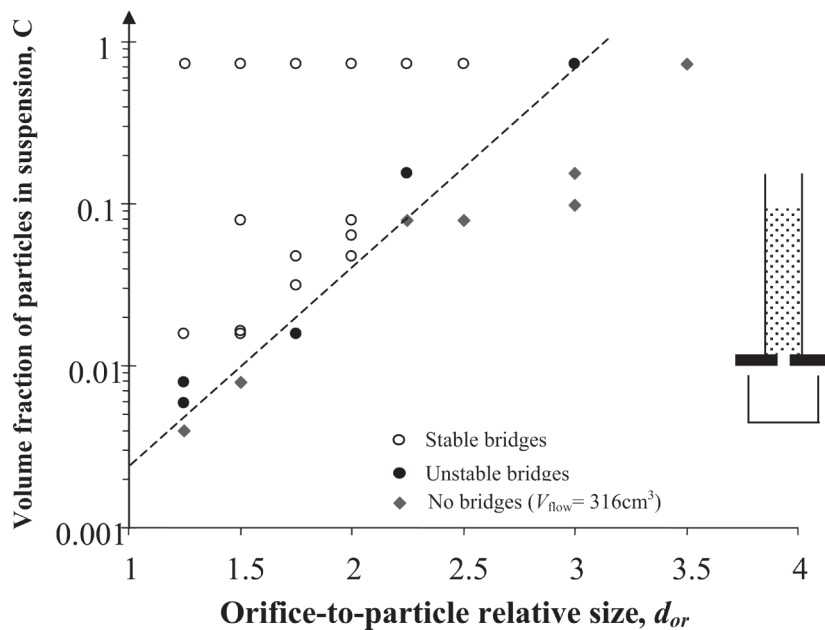


Fig. 3—Particulate bridge formation: Dispersed particles in flowing fluid. Bridge formation depends on volume fraction  $C$  and relative size  $d_{or}/d_p$ . The probability of bridge formation increases with volume throughput. [Note: The experiment involves a stable suspension of Nylon particles in de-aired saltwater at matched mass density,  $\rho_f = \rho_p$ , that is allowed to flow through an orifice in the bottom plate (see schematic on the right)].

### Radial Clogging and Flushing

Radial flow is the prevailing flow condition in oil production operations. For a given flow rate  $q$ , the average fluid-flow velocity at a radial distance  $r$  is  $v = q/(2\pi r)$ . The following sequence of events is anticipated on the bases of results discussed above:

- A radially varying flow velocity implies a radially varying balance between particle-level forces (Figs. 1 and 3). It is anticipated that no particle transport will occur in the far field (large  $r$ , low  $v$ , and low  $Ar$ ); particle transport with gravity offset will prevail at intermediate radial distances (intermediate  $v$ ,  $Fr$ , and  $Re$ ); and inertial retardation aggravated by interparticle interactions

and fluid-flow disruption will take place in the near field (small  $r$ ; high  $v$ ,  $Fr$ , and  $Re$ ).

- The increasing retardation toward the well implies a gradual accumulation of particles (i.e., local increase in volume fraction).
- When bridging is mechanically possible [i.e.,  $d_o/d_p \leq \delta_{min}$  (see Fig. 2)], the increase in volume fraction of particles enhances the probability of bridging.
- Bridging of a pore throat causes an increase in adjacent flow velocities, promoting further clogging nearby.
- These observations suggest that bridging should initiate and propagate at a critical radial distance from the well.

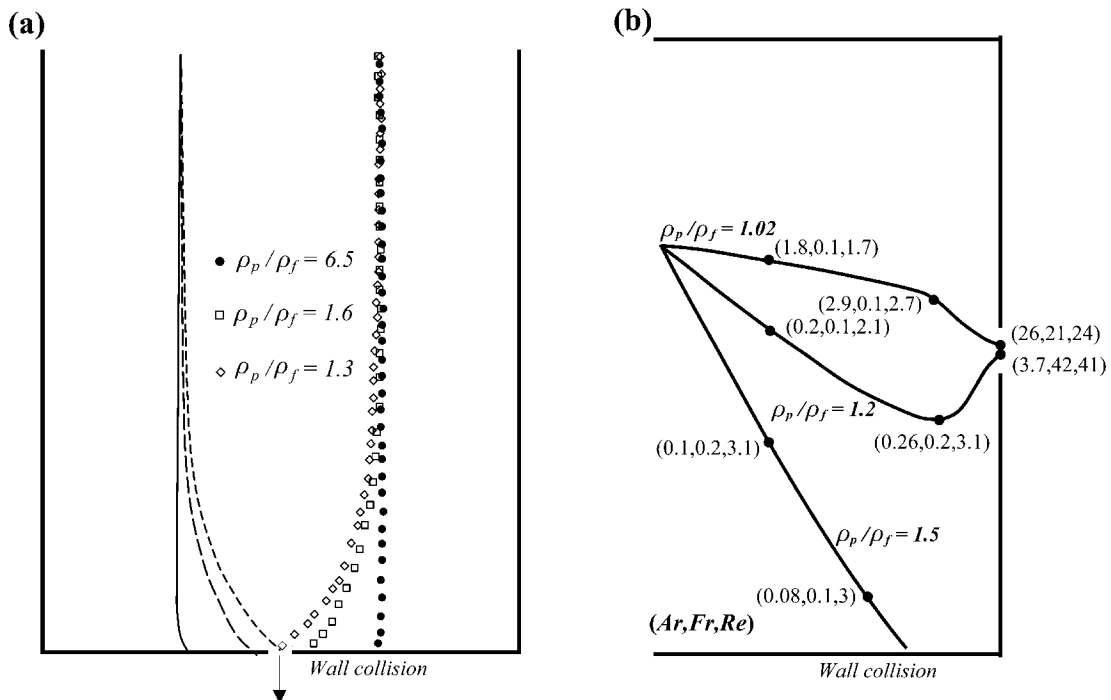


Fig. 4—Inertial retardation. The contrast between fluid and particle mass densities,  $\rho_p/\rho_f \neq 1$ , causes particle deviations from fluid lines. (a) Experimental study (points) and numerical verification (lines) for flow in the direction of gravity. (b) Numerical simulation for flow perpendicular to gravity.

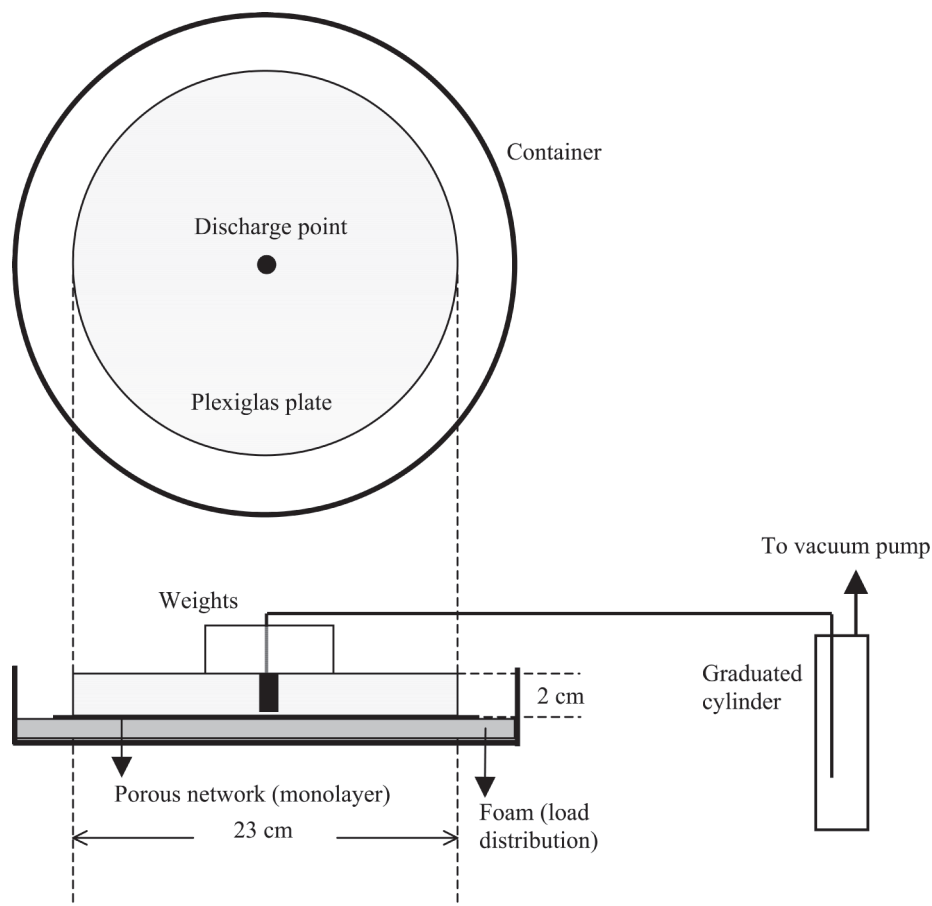


Fig. 5—Device used in radial clogging experiments.

The evolution of clogging in radial flow was investigated with a transparent network to facilitate the visualization of pore-level processes. The experimental device consisted of a rigid Plexiglas disk placed atop a monolayer of densely packed, mono-sized particles (size  $d_m=127\ \mu\text{m}$ ) cemented onto a bottom substrate (Fig. 5). Flow through the resulting interconnected porous network was imposed from the periphery to a central perforation. The fluid mixture consisted of oil and homogeneously mixed particles, with a particle volume fraction  $C=0.006$ . The size of migratory mineral particles ranged from a  $d_p(25\%)=6.5\ \mu\text{m}$  to  $d_p(75\%)=22\ \mu\text{m}$ , with a mean diameter  $d_p(50\%)=13\ \mu\text{m}$  [percentages refer to cumulative distribution (i.e., “smaller than”)]. The evolution of clogging was recorded with a digital video camera. Fig. 6 shows a sequence of redrawn top-view images for one of the tests, in which dark dotted regions represent particle accumulations. In all cases, clogging evolves into a self-stabilizing ring pattern that forms at a characteristic radial distance from the discharge point.

The following pore-level experimental observations were made: (a) Early migrating particles reach the discharge point and are removed soon after fluid flow is initiated; (b) particle bridges begin to form at a characteristic radial distance and align into small arches with endpoints typically facing the discharge point; (c) these clogging arches affect flow paths—it was common to see nearby particles migrating away from the central well; and (d) particle collisions and accumulations lead to the formation of new arches often linking existing ones, and to the additional accumulation of particles behind them. As these processes advance, arches grow in thickness and length and become interconnected, and the severity of clogging increases until the continuous annular clogging pattern is established (Fig. 6).

The cumulative throughput volume reflects the evolution of annular clogging, as shown in Fig. 7 for various tests conducted at

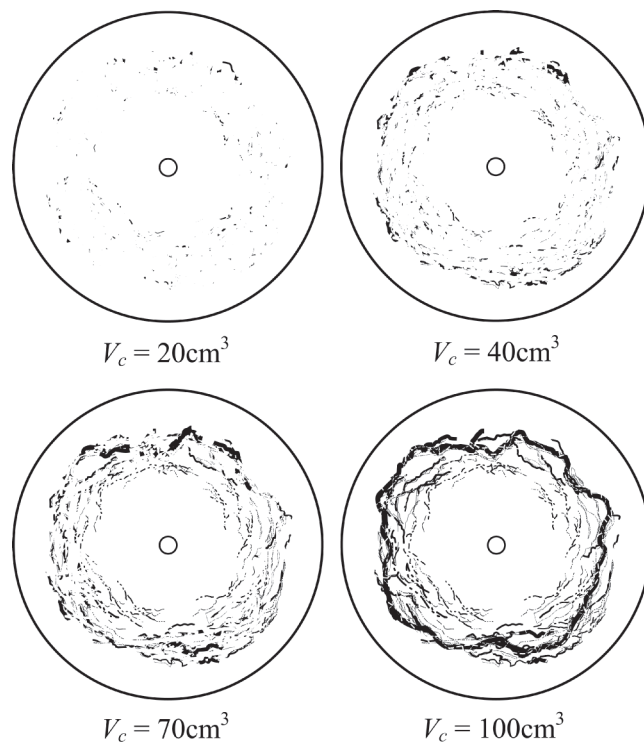


Fig. 6—Nonlinear particle-entrained radial fluid flow in porous networks: Self-stabilizing annular clogging ring in a clean porous network when  $d_o/d_p < \delta_{min}$  ( $V_c$ =pore fluid volume throughput; oil viscosity  $\mu=171\ \text{cp}$ ). Top view of the evolution of annular clogging (dark zones).

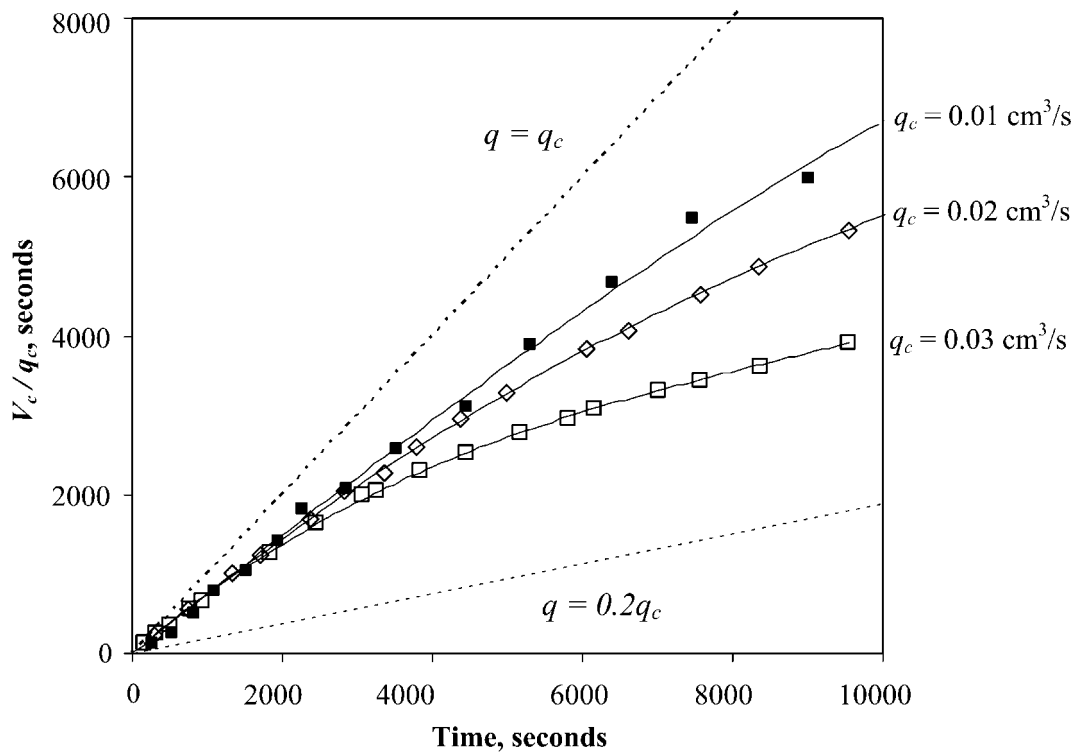


Fig. 7—Change in flow rate during clogging: Tests conducted at different gradients. The initial flow rate of particle-entrained fluid is similar to that of clean fluid  $q_c$  (without fines). Clogging progresses faster in time and requires a lower throughput volume  $V_c$  when the applied hydraulic gradient increases, as predicted by inertial retardation.

different hydraulic gradients. Flow rates drop from an initial value that corresponds to the flow rate of the fluid without particles  $q_c$  to a post-clogging flow rate smaller than  $q_c$  by a factor of five. All other parameters being constant, the data show that the development of clogging requires less time and a smaller throughput fluid volume when the applied gradient increases. In addition, the radius of the annular clogging ring decreases in agreement with retardation results.

A range of particle sizes was involved in this experiment; it is anticipated that larger particles form bridges first, leaving smaller pore throats for bridge formation by smaller particles. Such a recursive clogging phenomenon could lead to very low final flow rates.

For comparison, a similar device was used for a complementary flushing study. In this case, the porous network was a multilayer sand specimen (monosized,  $d_m = 310\mu\text{m}$ ) and much smaller particles [ $d_p = 13\mu\text{m}$  (i.e.,  $d_m/d_p = 24$ ,  $d_o/d_p \approx 6$ )] were mixed in with the sand during specimen preparation (mass fraction = 0.5%). The test was terminated when the increase in flow rate suggested piping by particle flushing. Then, the specimen was carefully disassembled to reveal the flushing pattern. In a stable flushing process, one would expect a cylindrical flushing front receding from the discharge point until the fluid velocity falls below the velocity required for particle mobilization. However, the development of unstable flushing with “finger-type” flow localization was observed; the high hydraulic gradient at finger tips caused flow velocities that sustain and guide particle flushing. Fig. 8 shows the top view of a disassembled specimen; fine-flushed regions are shown in white, while black zones correspond to fine-bearing sediments.

## Conclusions

The migration of particles through porous networks is controlled by particle-level forces. The interplay among participating forces results in distinctive phenomena that depend on the magnitude of local fluid and particle velocities, particle shape and concentrations, relative mass densities, and relative pore-throat size vs. migratory particle size.

In radial flow, particle-level phenomena associated with particle migration and retardation vary with radial distance from the discharge point (e.g., well) owing to the associated nonhomogeneous fluid-velocity profile. When conditions are appropriate for bridge formation (i.e.,  $d_o/d_p \leq \delta_{\min}$ ), particle transport in radial flow leads to a self-stabilizing clogging ring that forms at a characteristic radial distance. Conversely, unstable particle flushing and flow localization occur when the porous network contains particles that are much smaller than pore throats (i.e.,  $d_o/d_p \geq \delta_{\max}$ ).



Fig. 8—Nonlinear particle-entrained radial fluid flow in porous networks. Localized flushing and finger formation in a porous medium containing small mobile particles, where  $d_o/d_p > \delta_{\max}$ . Black represents the fine-bearing sediment, and white shows the fine-depleted zones.

## Nomenclature

- $C$  = volumetric particle concentration, ml/ml  
 $d_m$  = matrix particle diameter,  $\mu\text{m}$   
 $d_o$  = pore-throat size,  $\mu\text{m}$   
 $d_{or}$  = orifice size,  $\mu\text{m}$   
 $d_p$  = migratory particle diameter,  $\mu\text{m}$   
 $F$  = force, N  
 $g$  = gravity,  $\text{cm}/\text{sec}^2$   
 $q$  = flow rate,  $\text{cm}^3/\text{sec}$   
 $q_c$  = flow rate of fluid without particles,  $\text{cm}^3/\text{sec}$   
 $V_c$  = pore fluid volume throughput,  $\text{cm}^3/\text{sec}$   
 $\alpha$  = coefficient  
 $\beta$  = exponent  
 $\delta$  = size ratio  
 $\mu$  = fluid viscosity, cp  
 $v$  = velocity,  $\text{cm}/\text{sec}$   
 $\rho_f$  = fluid mass density,  $\text{g}/\text{cm}^3$   
 $\rho_p$  = particle mass density,  $\text{g}/\text{cm}^3$

## Acknowledgments

Support for this research was provided by Shell, the Natl. Science Foundation, and the Goizueta Foundation.

## References

- Beresnev, L.A. and Johnson, P.A. 1994. Elastic Wave Stimulation of Oil Production: A Review of Methods and Results. *Geophys.* **59**: 1000–1017.
- Bhatia, S.K., Moraille, J., and Smith, J.L. 1998. Performance of Granular vs. Geotextile Filters in Protecting Cohesionless Soils. *Filtration and Drainage in Geotechnical and Geoenvironmental Engineering*. ASCE Geotechnical Special Publication (78): 1–29.
- Bigno, Y., Oyeneyin, M.B., and Peden, J.M. 1994. Investigation of Pore-Blocking Mechanism in Gravel Packs in the Management and Control of Fines Migration. Paper SPE 27342 presented at the SPE Formation Damage Control Conference, Lafayette, Louisiana, 7–10 February.
- Bonala, M.V.S. and Reddi, L.N. 1998. Physicochemical and Biological Mechanisms of Soil Clogging—An Overview. *Filtration and Drainage in Geotechnical and Geoenvironmental Engineering*. ASCE Geotechnical Special Publication (78): 43–68.
- Cerda, C.M. 1987. Mobilization of Kaolinite Fines in Porous Media. *Colloids and Surfaces* **27**: 219–241.
- Goren, S. and O'Neill, M.E. 1971. On the Hydrodynamic Resistance to a Particle of a Dilute Suspension When in the Neighborhood of a Large Obstacle. *Chem. Eng. Sci.* **26**: 325–338.
- Gruesbeck, C. and Collins, R.E. 1982. Entrainment and Deposition of Fine Particles in Porous Media. *SPEJ* **22** (6): 847–856. SPE-8430-PA.
- Herzig, J.P., LeClerc, D.M., and LeGoff, P. 1970. Flow of Suspensions Through Porous Media—Application to Deep Filtration. *Ind. and Eng. Chem.* **62** (5): 9–35.
- Jones, Frank O. Jr. 1964. Influence of Chemical Composition of Water on Clay Blocking of Permeability. *JPT* **16** (4): 441–446; *Trans.*, AIME, **231**.
- Kennedy, T.C., Chahal, R., Chiu, E., Ofoegbu, G.I., Omenge, G.N., and Ume, C.A. 1985. Controlling Constriction Sizes of Granular Filters. *Canadian Geotech. J.* **22** (1): 32–43.
- Kennedy, T.C. and Lau, D. 1985. Internal Stability of Granular Filters. *Canadian Geotech. J.* **22** (2): 215–225.
- Khilar, K.C. and Fogler, H.S. 1998. *Migration of Fines in Porous Media*. Kluwer Academic Publishers: Dordrecht, The Netherlands.
- Kia, S.F., Fogler, H.S., and Reed, M.G. 1987. Effect of pH on Colloidally Induced Fines Migration. *J. Coll. Inter. Sci.* **118** (1): 158–168.
- McDowell-Boyer, L.M., Hunt, J.R., and Sitar, N. 1986. Particle Transport Through Porous Media. *Water Res. Research* **22**: 1901–1921.
- Muecke, T.W. 1979. Formation Fines and Factors Controlling Their Movement in Porous Media. *JPT* **31** (2): 144–150. SPE-7007-PA.
- Oyeneyin, M.B., Peden, J.M., Hosseini, A., and Ren, R. 1995. Factors to Consider in the Effective Management and Control of Fines Migration in High-Permeability Sands. Paper SPE 30112 presented at the SPE European Formation Damage Conference, The Hague, 15–16 May.
- Priisholm, S., Nielsen, B.L., and Haslund, O. 1987. Fines Migration, Blocking, and Clay Swelling of Potential Geothermal Sandstone Reservoirs, Denmark. *SPEFE* **2** (2): 168–178. SPE-15199-PA.
- Ramachandran, V., Venkatesan, R., Tryggvason, G., and Fogler, S. 2000. Low Reynolds Number Interactions Between Colloidal Particles Near the Entrance to a Cylindrical Pore. *J. Coll. Int. Sci.* **229**: 311–322.
- Raveendran, P. and Amiratharajah, A. 1995. Role of Short-Range Forces in Particle Detachment During Filter Backwashing. *ASCE J. Env. Eng.* **121** (12): 860–868.
- Reddi, L.N., Ming, X., Hajra, M.G., and Lee, I.M. 2000. Permeability Reduction of Soil Filters due to Physical Clogging. *J. Geotech. and Geoenv. Eng.* **126** (3): 236–246.
- Ryan, J.N. and Elimelech, M. 1996. Colloid Mobilization and Transport in Groundwater. *Colloids and Surfaces* **107**: 1–56.
- Sakthivadivel, R. and Einstein, H.A. 1970. Clogging of Porous Column of Spheres by Sediment. *ASCE J. of Hydraulic Eng.* **96** (2): 461–472.
- Santamarina, J.C. 2002. *Soil Behavior at the Microscale: Particle Forces, in Soil Behavior and Soft Ground Construction*. ASCE Geotechnical Special Publication **119**: 25–56.
- Sharma, M.M. and Yortsos, Y.C. 1987. Fines Migration in Porous Media. *AIChE J.* **33**: 1654–1662.
- Sharma, M.M., Chamoun, H., Sharma, D.S.H.S.R., and Schechter, R.S. 1992. Factors Controlling the Hydrodynamic Detachment of Particles From Surfaces. *J. Coll. Inter. Sci.* **149** (1): 121–134.
- Skempton, A.W. and Brogan, J.M. 1994. Experiments on Piping in Sandy Gravels. *Geotechnique* **44**: 449–460.
- Vaidya, R.N. and Fogler, H.S. 1990. Formation Damage due to Colloidally Induced Fines Migration. *Colloids and Surfaces* **50** (12): 215–229.
- Valdes, J.R. 2002. Fines Migration and Formation Damage—Microscale Studies. PhD dissertation, Georgia Inst. of Technology: Atlanta, Georgia.
- Wennberg, K.E. 1998. Particle Retention in Porous Media—Applications to Water Injectivity Decline. PhD dissertation, Norwegian U. of Science and Technology: Trondheim.

**Julio R. Valdes** is an assistant professor in the Dept. of Civil and Environmental Engineering at San Diego State U. He holds BSc, MSc, and PhD degrees in civil engineering, all from the Georgia Inst. of Technology (GIT). **J. Carlos Santamarina** is the Goizueta Foundation Chair Professor in the School of Civil and Environmental Engineering at GIT. Previously, he was with the U. of Waterloo, Waterloo, Ontario, Canada, and the Polytechnic U. in New York City. He holds an I. Civil degree from the U. Nacional de Cordoba, Argentina, an MSc degree from the U. of Maryland, and a PhD degree from Purdue U., all in civil engineering.